Solution Structure of Polymyxins B and E and Effect of Binding to Lipopolysaccharide: An NMR and Molecular Modeling Study‡

Primož Pristovšek† and Jurka Kidrič*

National Institute of Chemistry, Hajdrihova 19, 1000 Ljubljana, Slovenia

Received March 2, 1999

The cyclic decapeptides polymyxin B (**PmB**) and E (**PmE**) (mo-K′TK′-cyclo-[K′K′XLK′K′T]; mo, methyl octanoate; K′, diaminobutyric acid; X, D-Phe (**PmB**) or D-Leu (**PmE**)) display antimicrobial and lipopolysaccharide (LPS) antagonistic activities. We have investigated the conformational behavior of **PmB** and **PmE** in water solution, free and bound to LPS, by homonuclear NMR and molecular modeling methods. The free peptides exist in equilibria of fast exchanging conformations with local preferences for a distorted type II′ β-turn from residues 5−8, and/or a γ-turn in residue 10. These two motifs are not present in the bound conformation of the peptides. The latter is amphiphilic separating the two hydrophobic residues in the cycle from the positively charged diaminobutyric acid side chains by an envelope-like fold of the cycle. The bound conformation is used for the derivation of a model of the **PmB**−lipid A complex based on electrostatic interactions and reduction of hydrophobic area. The proposed mode of binding breaks up the supramolecular structure of LPS connected with its toxicity. The model should contribute to the understanding of entropy-driven **PmB**−lipid A binding at the molecular level and assist the design of inhibitors of endotoxic activity.

Introduction

Lipopolysaccharide (LPS) is the main constituent of the outer membrane of Gram-negative bacteria.[1] It is one of the major ligands recognized by the innate immune system and serves as a signal for cellular activation (most importantly of monocytes and macrophages), resulting in the release of cytokines and other mediators,[2] and triggering a cascade of defense reactions. At higher levels LPS may cause septic shock, a constellation of symptoms followed by multiple system organ failure that leads to death in 60% of the cases; its detoxification is therefore an interesting and urgent target. Recent approaches to develop molecules that neutralize endotoxin have concentrated on peptides that bind and detoxify LPS. These peptides are polymyxin B and synthetic peptides derived from it[3,4] and also fragments of proteins that bind LPS, e.g. LBP,[5,6] LALF,[6,7] TALF,[8] BPI,[6,9] and CAP37.[10]

LPS is an amphiphile consisting of the lipid A, a core oligosaccharide, and an outer polysaccharide composed of repeating hetero-oligosaccharide subunits; the lipid A is a hydrophobic, lipid-rich moiety that harbors the endotoxic principle of LPS and is the most highly conserved part of the structure, typically with two glucosamines, two phosphate esters, and six fatty acid chains[11] (Figure 1). It has been suggested that the bisphosphorylated hexosamine backbone of lipid A is essential for the specific binding of LPS, while the acylation pattern plays a critical role for LPS-promoted cell activation.[12]

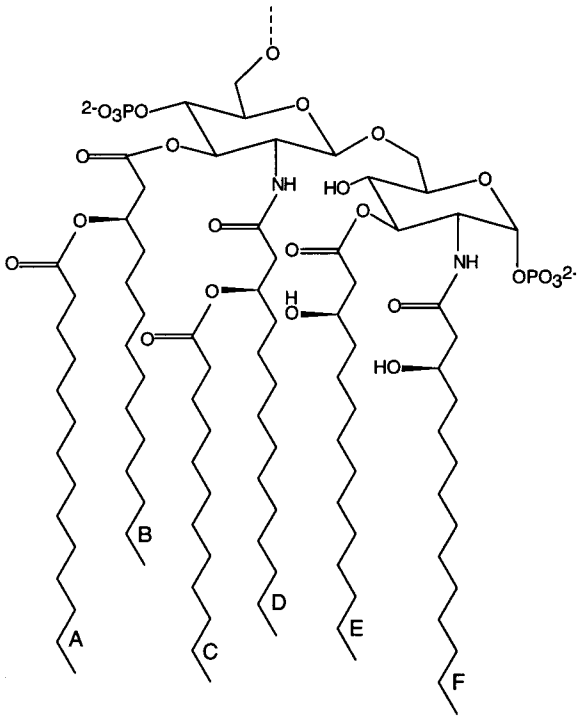

Figure 1. Structure of lipid A such as is found in *E. coli* strains; the fatty acid side chains are named with letters.

The amphiphilic character of LPS causes typical aggregate formation in water; this has been extensively investigated by various physical methods.[13] Solution NMR,[14−16] X-ray powder diffraction,[17,18] fluorescence resonance energy-transfer analysis,[19] neutron small-angle scattering,[20] and molecular modeling[17,21,22] have

* To whom correspondence should be addressed

† Presently on leave at the Institut für Biophysikalische Chemie, J.W. Goethe Universität, Marie Curie Strasse 9, 60439 Frankfurt, Germany.

‡ Abbreviations: 2D, two-dimensional; BPI, bactericidal/permeability increasing protein; CAP37, cationic antimicrobial protein of molecular mass 37 kDa; Dab, α,γ-diaminobutyric acid; DG, distance geometry; DQF-COSY, double-quantum filtered 2D correlation spectroscopy; K′, Dab; LALF, limulus anti-LPS factor; LBP, LPS binding protein; LPS, lipopolysaccharide; mo, methyl octanoate; NOE, nuclear Overhauser effect; NOESY, 2D NOE spectroscopy; PmB, polymyxin B; PmBN, polymyxin B nonapeptide; PmE, polymyxin E; rmsd, root-mean-square deviation; ROESY, rotating-frame 2D NOE spectroscopy; TALF, Tachypleus anti-LPS factor; TOCSY, 2D total correlation spectroscopy; TRNOE, transferred NOE experiment; WATERGATE, water suppression by gradient-tailored excitation.

10.1021/jm991031b CCC: $18.00
Published on Web 10/09/1999

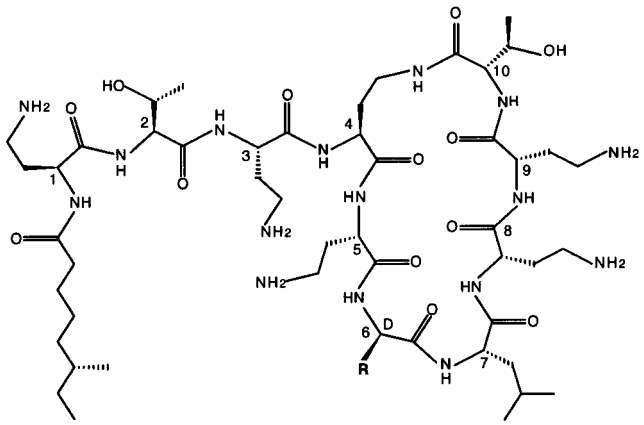

Figure 2. Molecular structure of polymyxins B (**PmB**, R: Phe side chain) and E (**PmE**, R: Leu side chain).

been applied to elucidate the three-dimensional structure of LPS, lipid A, and its aggregates.

The molecular determinants of specific binding of lipid A by the two groups of LPS-neutralizing peptides mentioned above have been investigated. An LPS binding motif consisting of alternating series of positively charged and hydrophobic residues of the peptides forming a positively charged amphipatic loop has been put forward based on the X-ray structure of LALF;[23] however, neither the three-dimensional structures of the peptides nor the structural aspects of the lipid A−peptide interaction at the atomic level are known. The existence of a common binding motif is indicated by the similarities in the primary sequences of the peptides; its elucidation is important for practical (detoxification of LPS) as well as general aspects.

Investigations of the interactions between LPS (or lipid A) and oligopeptides were motivated by the finding that polymyxin B (**PmB**, mo-K′TK′-cyclo-[K′K′fLK′K′T]; mo, methyl octanoate; K′, diaminobutyric acid (Dab); f, D-Phe; the cycle is closed between the side chain of Dab 4 and the main chain of Thr 10; Figure 2), a cyclic, cationic peptide antibiotic, binds to lipid A[24] with an apparent dissociation constant in the micromolar range[25] and neutralizes its pathogenicity. The antibiotic action of **PmB** could be accounted for by its ability to direct intermembrane exchange.[26] Polymyxin E (**PmE**, mo-K′TK′-cyclo-[K′K′lLK′K′T]; l, D-Leu; Figure 2) differs in only one amino acid residue at position 6 and displays similar biological functions; however, **PmB** but not **PmE** inhibits insulin-mediated hypoglycemia.[27] Unfortunately, **PmB** is toxic and cannot be used for therapy. Rustici et al. have synthesized a series of peptides designed to mimic the primary and secondary structure of **PmB** and tested them for binding and detoxification of LPS and lipid A;[4] they showed that multiple factors are responsible for optimal binding of peptide structures to lipid A, including the amphipatic and cationic features of the primary structure, the size of the structure, and the peptide conformation. Another study using linear polycationic amphiphilic peptides suggests that antibacterial and LPS neutralizing activities are dissociable.[28]

In contrast to the extensive spectroscopic and computer modeling investigations carried out on LPS and lipid A, little structural information obtained by spectroscopic methods exists for the peptides and the peptide−LPS or peptide−lipid A complexes. Initial NMR studies were focused on free **PmB** in water solution.[3,29] Conformations of **PmB** analogues in dimethyl sulfoxide from NMR spectra and molecular modeling have been proposed.[30] Recently, an NMR and molecular dynamics (MD) study of polymyxin B nonapeptide (PmBN), a **PmB** analogue lacking the mo-Dab 1 residue, has been published[31] and a model of the **PmB**−lipid A complex proposed that was based on the LPS-bound PmBN conformation derived from transferred NOE data and on electrostatic contacts of the γ-amino and the phosphate groups. However, a refined knowledge of interactions is desirable since the determination of the thermodynamic properties of LPS−**PmB** complexes using calorimetric titration clearly exposes the entropic drive to complexation,[32] thus confirming previous assumptions of its hydrophobic nature that were also proposed by Morrison et al.[24]

In this paper we present an NMR conformational study of **PmB** and **PmE** in water at room temperature, free and bound to LPS. In the first part of the study we show that numerous conformations of the seven-membered ring are possible that satisfy the NOE constraints obtained from the free peptides; the peptides most probably undergo fast conformational exchange. In the second part we use transferred NOE experiments of peptide−LPS mixtures introduced by Bhattacharjya et al.[31] in order to elucidate the bound conformations of **PmB** and **PmE** from the vastly increased number of restraints of the bound species; it turns out that the latter possesses an envelope-like bent ring conformation separating the hydrophobic and hydrophilic residues and rendering the structure amphiphilic. The bound conformation is used for docking to lipid A, and a model of the **PmB**−lipid A complex is derived; it is based on peptide−LPS contacts that (i) satisfy electrostatic attractions of the Dab γ-amino and the phosphate groups and (ii) reduce the hydrophobic area of both molecules exposed to the solvent. The model should contribute to the understanding of entropy-driven **PmB**−lipid A binding at the molecular level and assist the design of inhibitors of endotoxic activity.

Results

Conformational Analysis of Free Peptides in Water Solution. 1. NMR. The spin systems in the TOCSY spectra of **PmB** and **PmE** were assigned to the respective residues by taking into consideration the characteristic frequencies and numbers of resonances. The resonances of the five Dab residues are fairly well-resolved at 25 °C with the exception of Dab 1 and 5 in **PmB** that exactly coincide in the amide and α-proton resonances (Figure 3a, Table 1). The spin system of Dab 4 could be distinguished from the Dab residues 1, 3, 5, 8, and 9 by the resonance of its side chain amide proton. The sequential assignment was achieved using $d_{\alpha N}(i,i+1)$ and $d_{\beta N}(i,i+1)$ connectivities in the ROESY and NOESY spectra. The proton chemical shifts in **PmB** and **PmE** do not differ significantly in the residues that are common to both. The same is true for the $^3J_{\alpha H,NH}$ coupling constants (Table 2) that are in the range of average values expected for flexible molecules.

The temperature dependencies of the amide proton chemical shifts at 1 mM concentration (Table 2) indicate

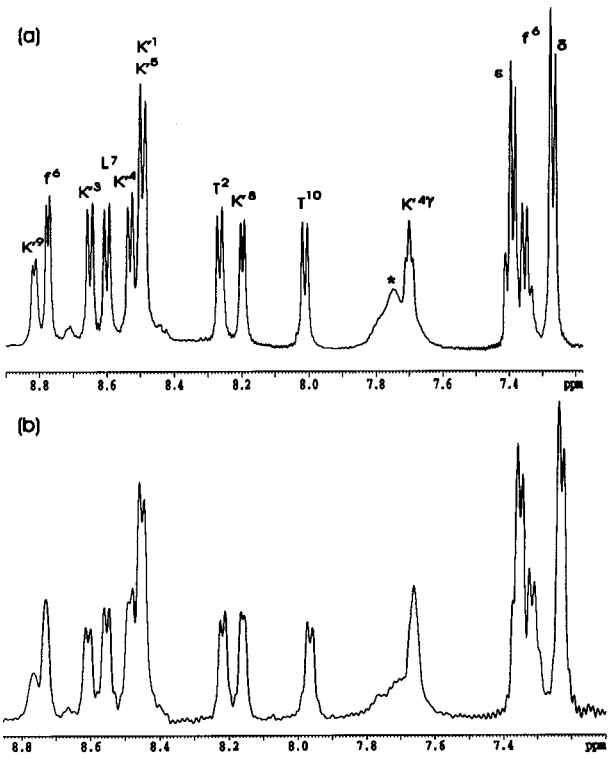

Figure 3. Amide and aromatic region of 1 mM **PmB** in 90% H_2O−10% D_2O at pH 4 and 25 °C (a) free and (b) in 8:1 w/w mixture with LPS.

Table 1. ^{1}H Chemical Shifts of 1 mM (a) **PmB** and (b) **PmE** in 90% H_2O−10% D_2O Mixture at pH 4 and 25 °C[a]

residue	HN	Hα	Hβ	Hγ	Hδ	others
			(a) **PmB**			
mo		2.29	1.55	1.09	0.80	
Dab 1	8.46	4.50	2.19, 2.05	3.07		
Thr 2	8.22	4.33	4.23	1.18		
Dab 3	8.61	4.49	2.20, 2.08	3.07		
Dab 4	8.49	4.24	1.90, 1.86	3.34, 3.13		HN γ 7.67
Dab 5	8.46	4.51	2.05, 1.97	2.92, 2.85		
D-Phe 6	8.73	4.49	3.12, 3.00		7.24	ϵ 7.36
Leu 7	8.56	4.16	1.45, 1.32	1.45	0.73, 0.65	
Dab 8	8.16	4.29	2.22	3.16, 3.12		
Dab 9	8.77	4.25	2.19	3.10		
Thr 10	7.97	4.15	4.24	1.18		
			(b) **PmE**			
mo		2.28	1.56	1.08	0.81	
Dab 1	8.46	4.48	2.15, 2.04	3.06		
Thr 2	8.17	4.33	4.22	1.17		
Dab 3	8.61	4.48	2.17, 2.09	3.06		
Dab 4	8.49	4.27	1.93, 1.84	3.31, 3.17		HN γ 7.78
Dab 5	8.51	4.54	2.13, 2.02	3.01		
D-Leu 6	8.58	4.26	1.62	1.54	0.89, 0.86	
Leu 7	8.71	4.38	1.64	1.56	0.89, 0.84	
Dab 8	8.22	4.30	2.24, 2.16	3.11		
Dab 9	8.72	4.25	2.17	3.08		
Thr 10	7.87	4.18	4.19	1.17		

[a] Values given relative to the water resonance at 4.75 ppm.

that the Dab 8 and, less strongly, the Dab 4γ amide protons are the only ones protected from solvent in **PmB** as well as in **PmE** and are most probably engaged in intramolecular H-bonding; the proton acceptors are not evident from NMR parameters but could be deduced from NOE-restrained simulations (see below).

In the NOESY spectra only a few cross-peaks are present (Figure 4a); the peptides at 25 °C and 600-MHz proton frequency are found near the zero NOE regime that varies from positive in the N-terminal residue (cross-peaks negative with respect to the diagonal peaks,

Table 2. Temperature Coefficients of the Amide Proton Chemical Shifts and $^3J_{HN,H\alpha}$ of 1 mM (a) **PmB** and (b) **PmE** in 90% H_2O−10% D_2O Mixture at 25 °C[a]

	(a) **PmB**		(b) **PmE**	
residue	temp coeff (10^{-3} ppm/K)	^3J (Hz)	temp coeff (10^{-3} ppm/K)	^3J (Hz)
Dab 1	−3.9	7.0	−5.5	7.5
Thr 2	−4.6	7.0	−6.1	7.3
Dab 3	−4.0	7.5	−5.3	7.1
Dab 4	−4.8	6.9	−6.1	6.5
Dab 4γ	**−1.5**		**−1.7**	
Dab 5	−3.9	7.0	−4.2	7.8
D-R[b] 6	−5.5	5.2	−5.2	5.6
Leu 7	−5.6	8.2	−8.8	8.2
Dab 8	**−0.8**	5.9	**−1.4**	7.3
Dab 9	−3.7	7.4	−8.8	8.2
Thr 10	−2.9	7.2	−3.9	7.4

[a] The temperature coefficients denoting protection from solvent are marked in bold. [b] R: (a) Phe, (b) Leu.

e.g. mo CαH$_2$−Dab 1HN, Dab 1HN−Dab 1β, Dab 1HN−Dab 1γ) to negative in the seven-membered cycle (cross-peaks positive with respect to the diagonal). In the ROESY spectra the peaks were more numerous and of greater intensity (Figure 4b); the increased number of scans used for recording the ROESY spectra (96 compared to 64 for NOESY) partly compensated for its intrinsically lower sensitivity. The NOE pattern obtained is shown in Figure 5a; it contains mainly intraresidual and sequential connectivities; no longer-range NOEs were observed except the weak NOE between Phe 6α and Dab 8HN. The NOE pattern of **PmE** turned out to be essentially identical and showed no significant differences in the parts that are common to both molecules (data not shown).

2. Molecular Modeling. The number of NOE distance restraints obtained from the ROESY spectra was 43 and 46 for **PmB** and **PmE**. A distance geometry, optimization, and energy minimization protocol was performed that resulted in 100 minimized structures. For both peptides a large number of different conformations of the seven-membered cycle were found that were all in fair agreement with the NOE constraints (maximum 0.12 Å violation per restraint and maximum violation below 1 Å). The distribution of the ϕ/ψ dihedral angles of residues 4−10 in the 10 best structures of **PmB** is shown in Figure 6a; significant variations are observed with nearly all residues. In some of the structures residues Dab 9 and Thr 10 are found in forbidden regions of the Ramachandran plot (see lower right quadrant of Figure 6a). D-Phe 6 is consistently found in the same region; however, the latter is forbidden for L but not for D amino acids since the ϕ,ψ map is inverted upon changing the chirality.

Although the peptides turned out to be quite flexible, a number of structures adopt a common local conformation characterized by a distorted type II′ β-turn extending from residues 5−8 or an inverse γ-turn around residue 10. The NOEs supporting the existence of the β-turn are Leu 7HN−Dab 8HN (strong) and Phe 6α−Dab 8HN (weaker). Additionally, the temperature coefficients of Dab 8HN have the low values of −0.0008 and −0.0014 ppm/K in PmB and PmE, respectively. These circumstances present the majority of the complementary pieces of evidence required for allowing the conclusion that a population of true turn conformations exists in aqueous solution.[33] Two of the best structures of **PmB**

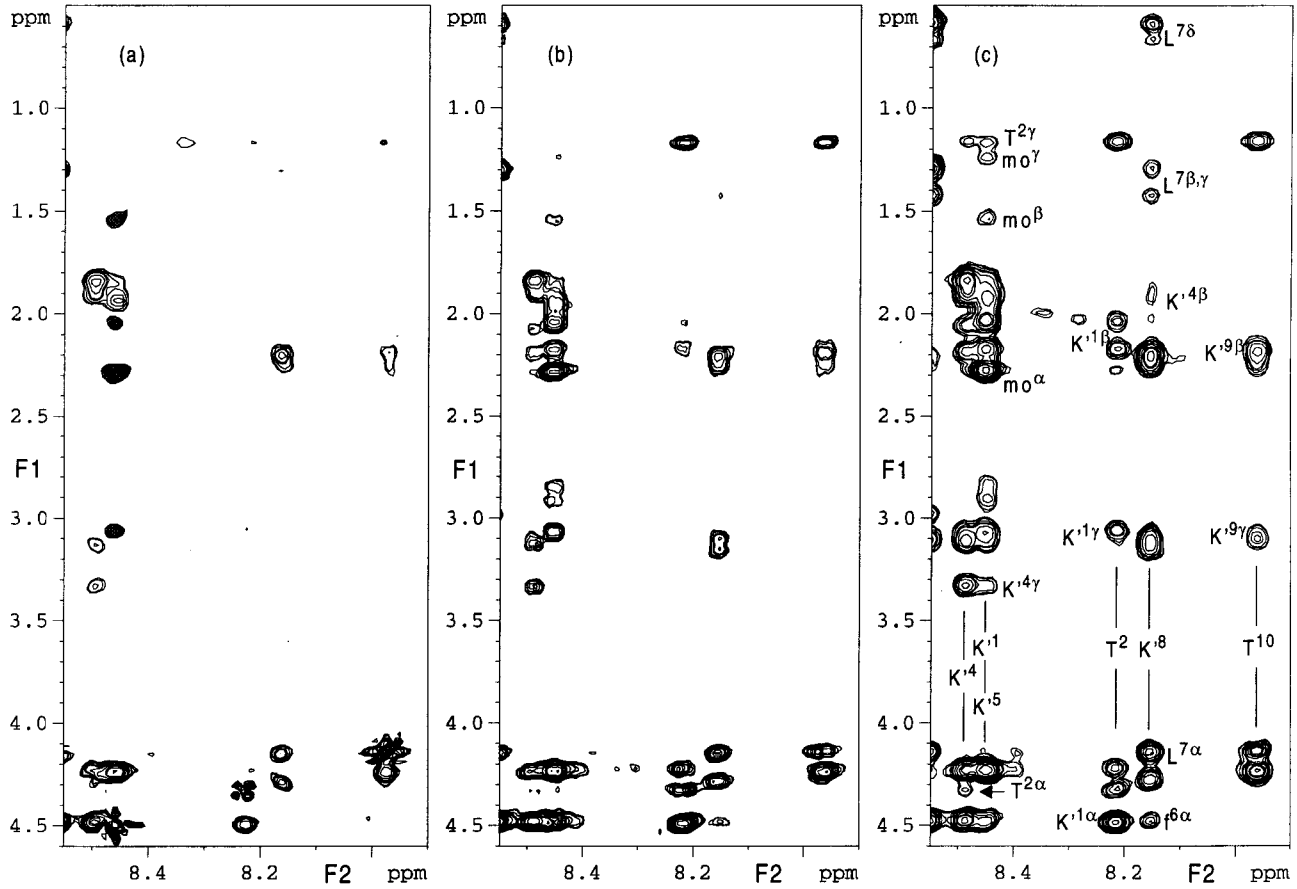

Figure 4. Fingerprint and aliphatic regions of two-dimensional spectra of 1 mM **PmB** in 90% H_2O−10% D_2O at pH 4 and 25 °C: (a) NOESY, mixing time 200 ms, positive peaks (with respect to the diagonal) are shown as multilevel contours and negative peaks as filled single contours; (b) ROESY, mixing time 200 ms, only negative peaks are shown; (c) 2D transferred NOE spectra of a 8:1 w/w PmB−LPS mixture, mixing time 200 ms, only positive peaks are shown. The amide proton assignment in F2 is given between vertical lines while the assignment along F1 is put beside the peak.

Table 3. Values of the ϕ and ψ Dihedral Angles of Residues 4−10 Spanning the Seven-Membered Cycle of Selected **PmB** and **PmE** Structures[a]

angle	(a)	(b)	(c)	(d)	(e)
ϕ^4	−85	−148	−79	−76	−90
ψ^4	72	26	154	−47	161
ϕ^5	−125	−164	−135	−148	−140
ψ^5	110	155	82	82	117
ϕ^6	70	−45	56	67	48
ψ^6	−108	−66	42	10	29
ϕ^7	−95	−78	62	59	58
ψ^7	62	30	82	76	92
ϕ^8	−142	53	−93	−82	−141
ψ^8	132	64	−81	−69	−72
ϕ^9	−70	−132	−86	−103	−126
ψ^9	169	−94	−58	−76	106
ϕ^{10}	68	−52	−139	−152	78
ψ^{10}	−56	49	−9	64	−27

[a] (a,b) Two structures of **PmB** in water solution shown in Figure 7; (c,d) two structures of **PmB** bound to LPS shown in Figure 8; (e) structure of **PmE** bound to LPS shown in Figure 9.

displaying these local conformations are shown in Figure 7, and their ϕ,ψ dihedral angle values for residues 4−10 are listed in Table 3 (columns a and b, respectively). The type II′ β-turn is depicted in Figure 7a; it is distorted in the value of the $\psi_{\text{Leu 7}}$ dihedral angle.[34] The structure in Figure 7b displays the inverse γ-turn. The structures found for **PmE** show an equivalent variation of the torsion angles of the seven-membered cycle; the most favorable ones are not significantly different from those found for **PmB** and are not shown. No conformational preferences at all can be deduced for the linear N-terminal chain of residues 1−3 of **PmB** and **PmE**; it shows increased flexibility relative to the cyclic residues in agreement with the shorter local correlation times evident from the positive NOE regime that prevails in the N-terminus.

Studies of the LPS-Bound PmB and PmE. 1. NMR. The addition of LPS to aqueous solutions of **PmB** and **PmE**, respectively, leads to moderate line broadening at weight ratios of peptide−LPS between 12:1 and 8:1 (Figure 3b). The chemical shifts of the resonances and the temperature coefficients of the amide proton chemical shifts remain nearly unchanged during titration with LPS. A more dramatic effect is observed in the NOESY spectra of the mixtures that display a large increase in number and intensity of the signals (Figure 4c). The N-terminal residues 1−3 not included in the seven-membered cycle still do not exhibit any medium range constraints except the weak NOE Thr 2α−Dab 4HN, but they do lose the positive NOE regime. More importantly, a significant number of cross-peaks mainly involving the side chains of the heptacycle residues 4−10 do appear (Figure 5b). The most interesting cross-peaks are the ones between residues 4 and 8 (Dab 4β−Dab 8HN, see Figure 4c, and Dab 4γHN−Dab 8β) which are not observed in the spectra of the free peptides and indicate the existence of a fold of the heptacycle that is

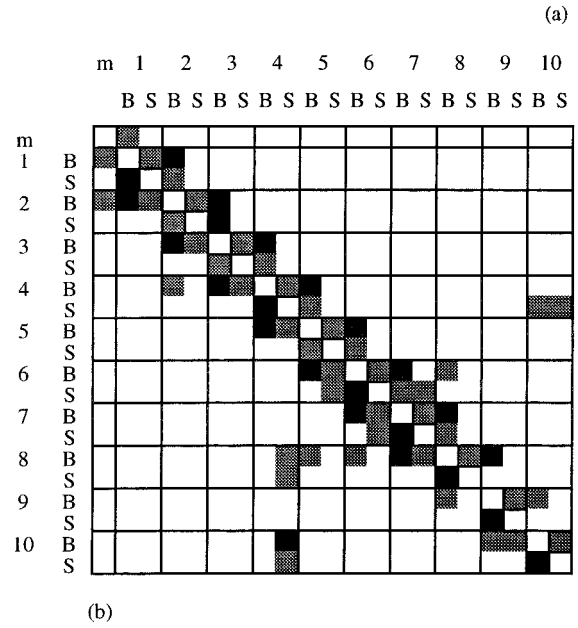

Figure 5. NOE connectivities of **PmB** at 1 mM concentration in water solution at 25 °C (a) free (upper triangle) and (b) in 8:1 w/w mixture with LPS (lower triangle). Each residue is numbered and divided in backbone (B) and side chain (S); m, methyl octanoate; black, strong NOE; gray, medium or weak NOE.

characteristic of the conformation bound to LPS. An equivalent pattern of NOEs is observed with **PmB** and **PmE** that differs only in some restraints involving Phe 6 and Leu 6, respectively.

2. Molecular Modeling. The number of NOE-derived distances was 93 and 96 for **PmB** and **PmE**, respectively. As expected, due to the limited number and mostly intraresidual/sequential character of the constraints observed with the first three N-terminal residues, no defined structure was obtained for the linear portion of the peptides; it is therefore not described in the following. The best 10 structures of **PmB** from the distance geometry and energy minimization protocol that was conducted with the full set of distance constraints can be divided in two families of conformations (Figure 8, top and bottom) that differ mainly in the orientation of the side chain of residue Dab 4 closing the cycle. The superimpositions of the backbone atoms of residues 4−10 of the members of the same families (rmsd from 0.18 to 0.50 Å) show their similarity, while the superimpositions between the structures from different families are larger (rmsd from 1.00 to 1.18 Å). Both families have a common global fold of the cycle characterized by a nearly 90° kink involving residues 5−8. In this arrangement the hydrophobic residues 6 and 7 are separated from the four hydrophilic Dab residues in the cycle. In addition, neither the distorted β-turn nor the γ-turn described for the free peptides are present in the bound conformation. The distribution of the ϕ/ψ dihedral angle values in residues 4−10 of the 10 best structures are shown in Figure 6b. Significant variations are observed only for residues 4 and 10 that span the region differing significantly in the two families. The ϕ/ψ values of Leu 7 cluster in the α_L region of the Ramachandran plot where none were found among the 10 best structures in the calculations involving the free peptides (Figure 6a); the same is true for

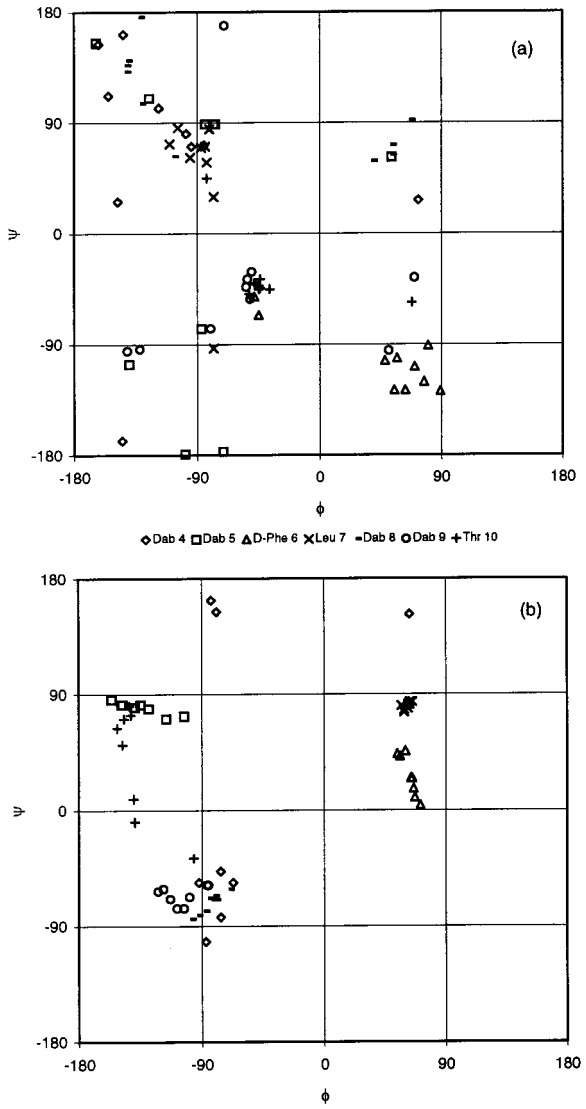

Figure 6. Ramachandran map of the backbone ϕ,ψ dihedral angles of residues 4−10 of **PmB** in the best 10 structures obtained with distance geometry using NOE distance restraints from (a) the free peptide and (b) the peptide in 8:1 w/w mixture with LPS.

D-Phe 6 that moved from the β to the α_R region. None of the residues are found in forbidden regions of the Ramachandran plot.

In the following we concentrate on the structures with the lowest potential energy inside each family that we refer to as the representative of the family. The energy of the representative structure of the first family (Figure 8, top) is lower by 11 kcal/mol than that of the second family (Figure 8, bottom). The values of the ϕ,ψ dihedral angles inside the seven-membered cycle of both representative structures are listed in Table 3, columns c and d, respectively.

Essentially the same observations were made with **PmE** and are therefore not repeated. The superimposition of the backbone atoms of residues 4−10 of the representative structures of the first families of **PmB** and **PmE** (rmsd 1.0 Å; Figure 9) shows their similarity. The values of the ϕ,ψ dihedral angles of the representative structure of **PmE** are listed in Table 3, column e.

In the following we concentrate on the representative of the first family (Figure 8, top) of conformations of

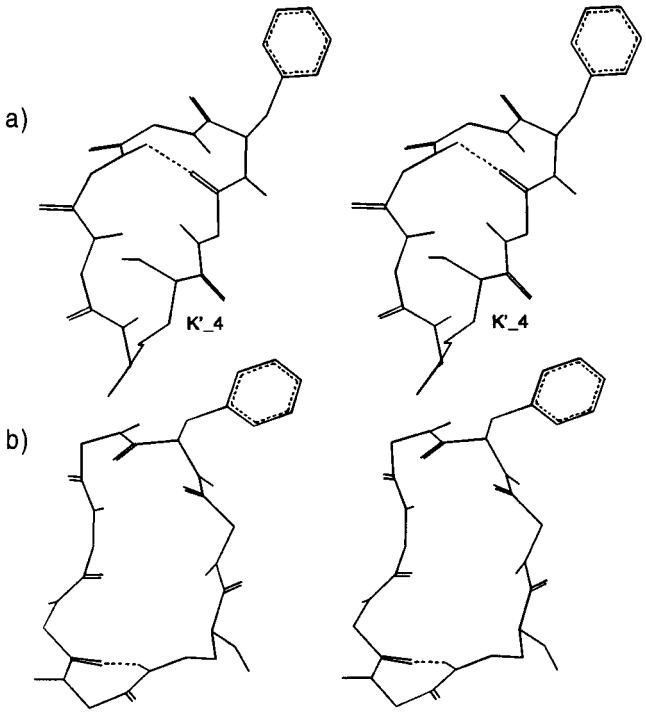

Figure 7. Stereoview of two selected structures of the seven-membered ring of **PmB** derived from distance geometry using NOE restraints from 1 mM PmB in 90% H_2O−10% D_2O at 25 °C: (a) distorted type II′ β-turn around residues 6 and 7 and (b) inverse γ-turn around residue 10. Only the backbone is displayed for clarity; the side chain of Phe 6 is shown for orientation; residue 4 is labeled. The H-bonds are shown as dotted lines.

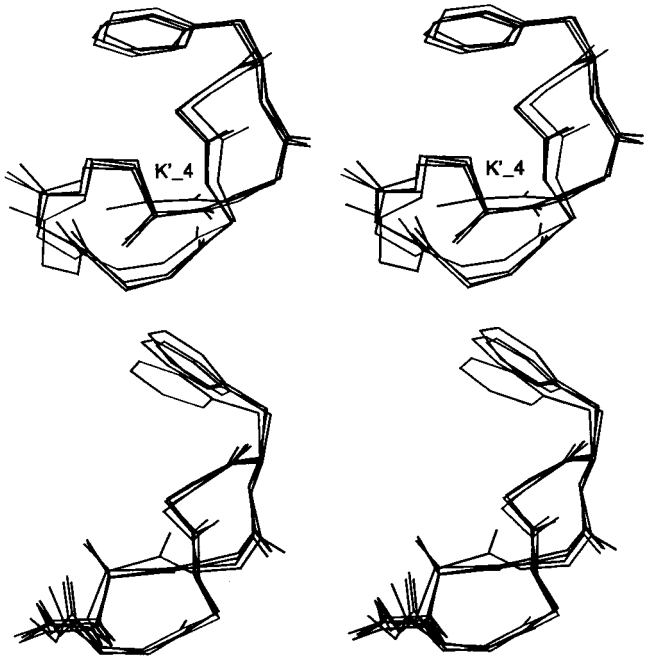

Figure 8. Stereoview of two families of structures of the seven-membered ring of **PmB** (rmsd for backbone atoms 0.18−0.22 and 0.24−0.50 Å) derived from distance geometry using NOE restraints from the 8:1 w/w **PmB**−LPS mixture in 90% H_2O−10% D_2O at 25 °C. Only the backbone is displayed for clarity; the side chain of Phe 6 is shown for orientation; residue 4 is labeled.

PmB bound to LPS and treat it as the representative of the polymyxin-type peptide conformations bound to LPS; it is lower in energy than the representative of the second family (Figure 8, bottom) and very similar to the representative structure of **PmE** bound to LPS.

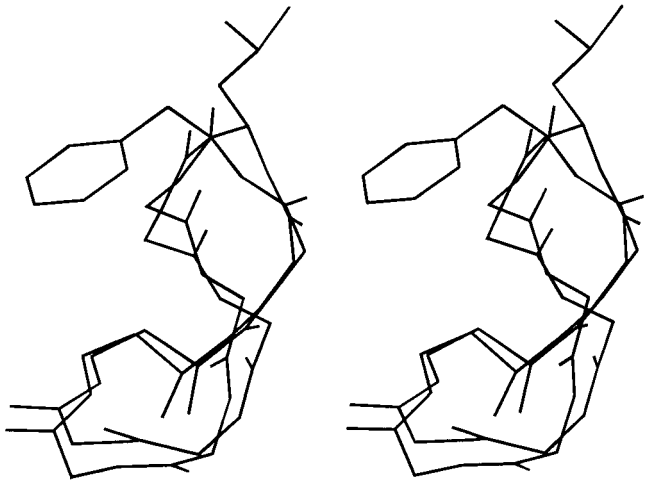

Figure 9. Stereoview of the superposition of the representative structures of the seven-membered ring of **PmB** and **PmE** derived from distance geometry using NOE restraints from the 8:1 w/w mixtures of the peptides with LPS in 90% H_2O−10% D_2O at 25 °C. The rmsd for backbone atoms is 0.99 Å. Only the backbone is displayed for clarity; the side chains of Phe 6 and Leu 6, respectively, are shown for orientation; Dab 4 is in front.

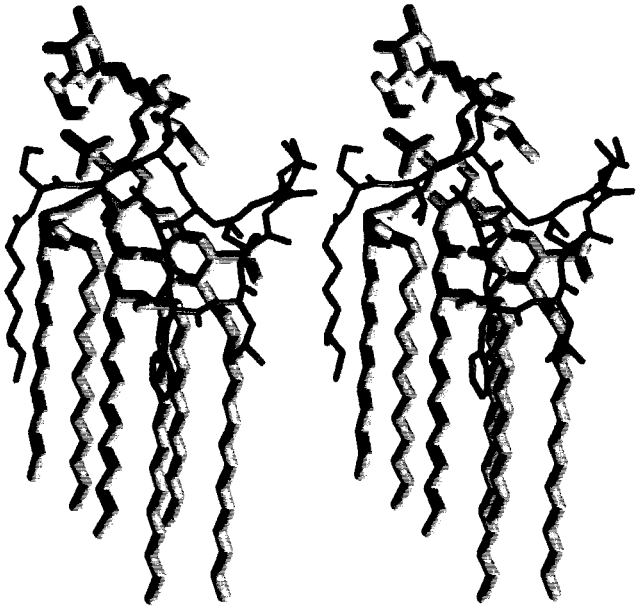

Figure 10. Stereoview of the proposed model of **PmB** docked to lipid A. Only heavy atoms are displayed for clarity. The conformation of the seven-membered cycle of **PmB** is taken from the representative structure (Figure 9).

3. Docking Studies of PmB with Lipid A. The representative structure of **PmB** was used for manual docking to the lipid A model. The **PmB** cycle was kept rigid in the conformation obtained from the NMR refinement, while all the side chains and the N-terminal residues 1−3 were free to move. The final model is displayed in Figure 10; the two phosphate groups of lipid A are in close contact with the positively charged side chains of Dab 1 and 5, and Dab 8 and 9, respectively; the Dab 3 side chain remains close to the polar sugar residues. The hydrophobic residue Phe 6 docks on the fatty acid side chains A and C of lipid A (Figure 1) and Leu 7 on C and F, while the N-terminal aliphatic chain

of the mo is in contact with A and B. The weak NOE Thr 2α−Dab 4HN that is observed in the NOESY spectra of the peptide−LPS mixtures is in agreement with the proximity of both protons in the docked model.

Discussion

PmB and **PmE** are two of the interesting examples of small molecules that display different NOE regimes in different parts of the molecule (Figure 4a). The negative regime is present in the greater part of the molecule (residues 2−10). The positive regime occurs at the border of the aliphatic and the peptidic moieties in the mo−Dab 1 sequence. It is most probably connected with the internal motions of aliphatic chains that are much faster than the ones in the polypeptide chains, leading to shorter correlation times. Similar observations were made in the case of the peptidoglycan muroctasin in dimethylsulfoxide that showed positive cross-peaks between the C-terminal lysine side chain and the attached stearoyl fatty acid chain.[35]

Throughout this study the similarity of the results with **PmB** and **PmE** is repeatedly mentioned; the similarity is not surprising taking into account that only one residue is different in the cyclic portion of the two molecules (Phe 6 in **PmB** compared to Leu 6 in **PmE**) but may lead to the question whether both molecules are really necessary to conduct this study. However, subtle differences in the physiological functions of **PmB** and **PmE** (see Introduction) do exist and lend each molecule its own importance; any conformational characteristics that are shared by both are possibly connected with common biological functions, i.e., detoxification of LPS, that are of interest in this study. The presence of two very similar molecules in the study is therefore important to allow us to isolate the common conformational features that possibly define the LPS binding motif of the polymyxin-type peptides. On the other hand, the subtle conformational differences between the two peptides (e.g. increased flexibility of the **PmE** ring relative to **PmB** due to the less bulky Leu 6 side chain) are not sufficient to understand the differences in their biological activities on a structural basis.

The free peptides in solution are structurally not well-defined. This was deduced from the absence of long- or medium-range NOEs and from the absence of J(HN,α) coupling constants >9 Hz or <5 Hz. However, there are experimental data (temperature coefficients of the amide proton chemical shifts, NOE pattern) supporting the existence of local conformational preferences, most notably the β-turn formed by residues 5−8. Usually β-turns in proteins appear at the surface and are therefore composed of hydrophilic residues in positions $i+1$ and $i+2$.[34] In decapeptides such as the polymyxins, all residues are at the surface, also the hydrophobic ones. The side chains of the two hydrophobic residues 6 and 7 tend to stay in proximity because of the hydrophobic effect. The proximity is proven by NOEs between the aromatic ring of Phe 6 and the methyls of Leu 7 in **PmB**. In the β-turn the distance between the two Cβ atoms (approximately 5 Å) always allows the mentioned proximity. We propose that this tendency of the hydrophobic side chains may promote the β-turn and is stronger with the aromatic chain of Phe 6 in **PmB** than with Leu 6 in **PmE**, as indicated by the higher absolute value of the temperature coefficient of Dab 8HN in **PmE**. We call this conformational motif "local" in order to emphasize that the conformation of the seven-membered cycle outside of the described region is not defined.

The cyclization of residues 4−10 does restrict the conformational space but leaves many possibilities to satisfy the NOE restraints without significantly increasing the potential energy. In this regard the polymyxins present an interesting novel type of seven-membered peptidic cycle that is closed via the side chain of the less common Dab amino acid. Some residues in the cycle of the best 10 structures of the free peptides are found in sterically forbidden regions of the Ramachandran plot (e.g. Dab 9 and Thr 10 in the right lower quadrant of Figure 6a). This could be connected with the steric constraints imposed upon the backbone by the seven-membered cycle. However, the cycle is large enough to allow relaxation of steric strain, as shown by the bound conformations. The occurrence of residues in the forbidden regions is more probably the consequence of the use of conflicting distance restraints in the simple DG protocol. The measured NOEs are averaged over an entire ensemble. The use of all NOE distance restraints arising from different conformations on a single molecule may lead to problematic or erroneous structures. However, the solution structures of the free peptides per se are not of particular importance for this paper and will be presented elsewhere, along with a detailed analysis of the conformational characteristics of the polymyxin-type cycle. The reason in the present paper we still use the protocol suitable for well-structured molecules is to allow direct comparison with the data obtained for the bound peptide. The latter are calculated with twice the number of NOE distance restraints but have neither significant NOE distance violations nor problems in the Ramachandran plot (Figure 6b). This is an indication that no conflicting distance constraints have been used and that the NOEs, although more numerous, in this case originate from a single family of structures.

In this light it is interesting to look again at the two representative structures of **PmB** bound to LPS (Figure 8). Not surprisingly the main differences appear in the most flexible part of the cycle, i.e., the side chain of Dab 4. The difference in energy (11 kcal/mol) may appear large enough to discard the second family from consideration as an alternative solution; it is not so in our opinion because the energies are calculated in vacuo and thus do not represent the true environment of the structures.[36] However, the region where the differences occur is weakly defined by NOE restraints, and the representative structure with lower energy is preferred.

The representative structure has an envelope-like bent cycle that separates the two hydrophobic residues 6 and 7 from the charged Dab residues 4, 5, 8, and 9 clustering on the lower side of the cycle and lends it a clearly amphiphilic character. The structure does not display any intramolecular H-bonding, including the prominent β- and γ-turns. The former was first proposed in the very early work by Chapman.[3] In the study involving PmBN both turns were described and reported as preserved upon binding to LPS.[31] This is not confirmed for **PmB** and **PmE** in the present study. How-

ever, the reorientation of the backbone necessary to go from the preferred solution structures displayed in Figure 7 to the bound conformation in the restricted cyclic system is not large and may occur rapidly in a suitable environment. The protection from solvent of the Dab 4γ and Dab 8 amide protons indicated by the temperature coefficients is connected with the free, nonbound species that still prevails in the mixture due to the higher concentration of peptide molecules relative to LPS and the relatively weak complex with LPS. This is also the reason the values of the coupling constants measured in the mixtures with LPS are not necessarily connected with the bound species and were not used for structure refinement. Such a caution was not necessary with the transferred NOEs because they originate from the bound species and are much stronger than the ones from the free species.[37]

The question appears whether the conformation found upon binding to LPS is not present in the free species or is simply not observable in the NOE patterns because of the proximity to the zero NOE regime. The ROESY spectra, although intrinsically less sensitive, do not show any trace of the very important connectivities between residues 4 and 8 for the free peptides. This indicates that the free peptides do not prefer the bound conformation, most likely because of the extreme exposure of the hydrophobic residues to the solvent that is entropically unfavorable.

In the study involving PmBN[31] no major changes of the peptide backbone upon titration with LPS were described although a number of additional backbone-to-side chain and inter-side-chain constraints were observed. Most importantly, the Dab 4−Dab 8 contacts were not observed. The reason may be a weaker complex of PmBN with LPS because of the missing N-terminal aliphatic chain or simply the inferior sensitivity of the 400-MHz spectrometer used in that study.

LPS has a very low critical micellar concentration (below 10^{-7} M)[38] and forms aggregates in the mixtures used for measurements. **PmB** influences the shape of the supramolecular structures of LPS, as demonstrated recently by dynamic light scattering techniques.[39] The stoichiometric ratio for the binding of **PmB** to LPS was found to lie between 0.6 and 1.0, as determined by calorimetric titrations.[39] The 1:1 docking model described in our paper is therefore in agreement with these experimental data.

During the docking an attempt was made to find the optimal contact of the positively charged Dab side chains with the negatively charged phosphate groups of lipid A; such contacts increase the enthalpy of binding and are observed in, e.g., proteins docked to membrane surfaces.[40] The importance of electrostatic interactions for **PmB**−LPS binding also is evident from its inhibition by divalent cations and high ionic strength.[41] On the other hand, the hydrophobic part of **PmB** (N-terminal mo aliphatic chain and residues 6 and 7) should be in contact with the lipophilic part of lipid A, i.e., the fatty acid chains. Such modes of binding are well-known from proteins that bind fatty acids, e.g., the lipases,[42,43] and are important for reduction of the hydrophobic area exposed to water; the latter would also rationalize the entropy-driven binding of the polymyxins to LPS.[32] In a recent biophysical study[39] specific interactions of **PmB** with LPS were indicated and a two-step mechanism for this interaction was proposed: electrostatic attraction between charged parts of the molecules and, in the second step, hydrophobic interactions between the nonpolar parts of both compounds.

On the basis of the obtained molecular model of the **PmB**−lipid A complex, we propose the following mode of the detoxifying action of the polymyxins. The supramolecular architectures (geometry and alkyl chain packing) of LPS are the critical determinants of their biological activity that might be mediated by some bulk colligative property in which the fatty acid chain packing plays a critical role; this is supported by the fact that LPS which lack even one fatty acid chain are not toxic.[44] The binding of polymyxins to the fatty acid chains of LPS in the way proposed in our model would disrupt any regular packing of LPS and thus render it inactive. Such a mode of action of the polymyxins can be effective even if the complexes are neither strong nor long-lived.

Conclusion

Polymyxins B (**PmB**) and E (**PmE**) were studied in aqueous solution using NMR and molecular modeling techniques. The free peptides exist in an equilibrium of fast exchanging conformations; only local conformational preferences can be deduced from NMR data and NOE restrained structure calculations, e.g., a distorted type II′ β-turn extending from residues 5−8 and/or a γ-turn in residue 10. In the mixtures of peptides with LPS complexes are formed that can be studied with transferred NOE experiments. A significantly increased set of intramolecular NOEs from the bound species enabled us to propose the bound conformation of **PmB** and **PmE**. It turned out to be amphiphilic clearly separating the two hydrophobic residues in the seven-membered cycle from the positively charged Dab side chains by an envelope-like fold of the cycle. Both turns indicated for the free peptides are lost. A model of the peptides bound to lipid A is proposed that covers the phosphate groups of the latter by the Dab side chains and the fatty acid chains by the N-terminal aliphatic chain and the two hydrophobic residues 6 and 7 in the cycle. Such a complex decreases the total hydrophobic area of both molecules and thus explains the entropy-driven binding of the polymyxins to LPS.[32]

On the basis of the molecular model of the complex, we propose that the detoxifying effect of the polymyxins is caused by breaking up of the supramolecular structure of LPS that is connected with its toxic action;[44] the regular arrangement of the fatty acid chains is disrupted by the inserted peptide molecules. A similar mode of action can also be proposed for the peptides derived from proteins that bind LPS and exhibit detoxifying effects.[5,10] A study involving some of these peptides is underway in this laboratory and will be reported elsewhere.

Experimental Section

NMR. PmB sulfate and **PmE** methanesulfonate salts were purchased from Fluka. The NMR spectra were obtained in 90% H_2O−10% D_2O solution at peptide concentrations 5−1 mM. The concentration dependence of the chemical shifts shows that the tendency for aggregation is already present at concentrations above 3 mM; for this reason the NOE measure-

ments were performed at 1 mM. All experiments were performed at pH 4 (adjusted by adding small quantities of 0.1 M HCl); under these conditions the possibility of peptide aggregation is reduced because of the protonation of the Dab γ-amino groups. LPS from *E. Coli*, Serotype 055:B5, was obtained from Fluka; the concentrations of LPS are given in mass per volume because of the heterogeneity of the polysaccharide outer core.

The assignment of ^{1}H resonances was performed using standard DQF-COSY,[45] TOCSY[46] (mixing time 70 ms), and two-dimensional NOE experiments (NOESY[47] and ROESY,[48] mixing times 200 ms) on a Varian Inova 600 spectrometer; data matrices of 2048 detected and 512 (1024 for DQF-COSY) indirect data points with 64 (96 for ROESY) scans were recorded and processed using a 90° shifted sine bell window function (180° for DQF-COSY). Water signal suppression was achieved by presaturation or with WATERGATE.[49] The temperature coefficients of the amide proton chemical shifts were calculated from one-dimensional experiments performed at different temperatures in the range 20−35 °C.

The binding of **PmB** and **PmE**, respectively, to LPS was followed by line broadening experiments where small aliquots (10 μL) of a concentrated stock solution of LPS (10 mg/mL in H_2O) were added to the 1 mM solutions of both peptides. Two-dimensional transferred NOE (TRNOE) experiments[37,50] with mixing times of 200 ms were carried out using mixtures of **PmB** and LPS that correspond to 15:1, 11:1, and 8:1 w/w ratios of both components; these conditions yield barely observable (15:1) to moderately broadened (8:1) lines of PmB. The mixture of **PmE** and LPS was only studied at 8:1 w/w ratio that corresponds to approximately 20:1 molar ratio.

Computational Methods. The three-dimensional structures of **PmB** and **PmE** were computed using the distance geometry program DG-II of the NMRefine module of Insight-II (MSI, 9685 Scranton Rd, San Diego, CA 92121-3752A) on a Silicon Graphics Indigo II workstation. The NOEs were classified as strong, medium, and weak, corresponding to distances of 2.5, 3.2, and 4 Å, respectively, based on the volumes of the assigned cross-peaks in the NOESY and/or ROESY spectra. The Dab 4γ−Dab 4γ' cross-peak was used for distance calibration; 50−100 different structures obtained by distance geometry were then optimized by simulated annealing. They were energy-minimized with DISCOVER using NOE distance restraints in the consistent valence force field (cvff[51]). The Dab side chains were kept uncharged in order to avoid charge repulsive effects; a distance-dependent dielectric constant was employed in order to simulate, at least in part, electrostatic screening by the solvent. The resulting structures were analyzed for the agreement with the NOE distance restraints, the values of the main chain dihedral angles, and H-bond pattern; a geometric criterion was used to check for the existence of H-bonds (d(O···H−N) < 2.3 Å, θ(O,H,N) > 120°).

The optimized coordinates of lipid A[22] were used for manual docking of the **PmB** model. Its seven-membered cycle was kept rigid in the conformation obtained from the NMR structure refinement using the data from the TRNOE experiments; the coordinates of lipid A were kept fixed.

The **PmB** model was brought in contact with the lipid A molecule from six different directions of approach. Each time a 100-ps molecular dynamics run at 300 K was started after an initial energy minimization, and 100 structures were sampled that were later energy-minimized. The final model was chosen on the basis of optimal intermolecular interaction energy of **PmB**. A detailed account of the docking procedure will be published elsewhere.

Acknowledgment. We are greatly indebted to Prof. D. Hadži for stimulating this work and for fruitful discussions. We are grateful to Dr. M. Kastowsky (Institute for Crystallography, Berlin) for the coordinates of lipid A and Dr. R. Jerala (National Institute of Chemistry, Ljubljana) and Dr. L. Franzoni (University of Parma, Parma) for critical reading of the manuscript. We thank Mr. Č. Podlipnik (Faculty of Chemistry, Ljubljana) for technical assistance and I. Tasić for careful preparation of the samples. This work was supported by the Ministry of Science and Technology of the Republic of Slovenia; P.P. is presently a Humboldt fellow and wishes to thank Prof. Dr. H. Rüterjans (Institut für Biophysikalische Chemie, Frankfurt) for his hospitality and permission to use the computer facilities of his lab.

Supporting Information Available: Coordinates of **PmB** docked to lipid A in PDB format. This material is available free of charge via the Internet at http://pubs.acs.org.

References

(1) Fearon, D. T.; Locksley, R. M. The instructive role of the innate immunity in the acquired immune response. *Science* **1996**, *272*, 50−54.
(2) Ulevitch, R. J.; Tobias, P. S. Recognition of endotoxin by cells leading to transmembrane signaling. *Curr. Opin. Immunol.* **1994**, *6*, 125−130.
(3) Chapman, T. M.; Golden, M. R. Polymyxin B. NMR evidence for a peptide antibiotic with folded structure in water. *Biochem. Biophys. Res. Commun.* **1972**, *46*, 2040−2047.
(4) Rustici, A.; Velucchi, M.; Faggioni, R.; Sironi, M.; Ghezzi, P.; Quataert, S.; Green, B.; Porro, M. Molecular mapping and detoxification of the lipid A binding site by synthetic peptides. *Science* **1993**, *259*, 361−365.
(5) Taylor, A. H.; Heavner, G.; Nedelman, M.; Sherris, D.; Brunt, E.; Knight, D.; Ghrayeb, J. Lipopolysaccharide (LPS) neutralizing peptides reveal a lipid A binding site of LPS binding protein. *J. Biol. Chem.* **1995**, *270*, 17934−17938.
(6) Battafarano, R. J.; Dahlberg, P. S.; Ratz, C. A.; Johnston, J. W.; Gray, B. H.; Haseman, J. R.; Mayo, K. H.; Dunn, D. L. Peptide derivatives of three distinct lipopolysaccharide binding proteins inhibit lipopolysaccharide-induced tumor necrosos factor-alpha secretion in vitro. *Surgery* **1995**, *118*, 318−324.
(7) Ried, C.; Wahl, C.; Miethke, T.; Wellnhofer, G.; Landgraf, C.; Schneider-Mergener, J.; Hoess, A. High affinity endotoxin-binding and neutralizing peptides based on the crystal structure of recombinant limulus anti-lipopolysaccharide factor. *J. Biol. Chem.* **1996**, *271*, 28120−28127.
(8) Kloczewiak, M.; Black, K. M.; Loiselle, P.; Cavaillon, J. M.; Wainwright, N.; Warren, H. S. Synthetic peptides that mimic the binding site of horseshoe crab antilipopolysaccharide factor. *J. Infect. Dis.* **1994**, *170*, 1490−1497.
(9) Gray, B. H.; Haseman, J. R.; Mayo, K. H. B/PI-derived synthetic peptides: synergistic effects in tethered bactericidal and endotoxin neutralizing peptides. *Biochim. Biophys. Acta* **1994**, *1244*, 185−190.
(10) Pereira, H. A.; Erdem, I.; Pohl, J.; Spitznagel, J. K. Synthetic bactericidal peptide based on CAP37: a 37-kDa human neutrophil granule-associated cationic antimicrobial protein chemotactic for monocytes. *Immunology* **1993**, *90*, 4733−4737.
(11) Rietschel, E. T.; Brade, L.; Holst, O.; Kulshin, V. A.; Lindner, B.; Moran, A. P.; Schade, U. F.; Zaehringer, U.; Brade, H. Molecular structure of bacterial endotoxin in relation to bioactivity. In *Cellular and molecular aspects of endotoxin reactions*; Nowotny, A., Spitzer, J. J., Ziegler, E. J., Eds.; Elsevier Science Publishers B.V.: Amsterdam, 1990; pp 15−32.
(12) Kirikae, T.; Schade, F. U.; Zaehringer, U.; Kirikae, F.; Brade, H.; Kusumoto, S.; Kusama, T.; Rietschel, E. T. The significance of the hydrophilic backbone and the hydrophobic fatty acid regions of lipid A for macrophage binding and cytokine induction. *FEMS Immunol. Med. Microbiol.* **1994**, *8*, 13−26.
(13) Seydel, U.; Labischinski, H.; Kastowsky, M.; Brandenburg, K. Phase behaviour, supramolecular structure, and molecular conformation of lipopolysaccharide. *Immunobiology* **1993**, *187*, 191−211.
(14) Zaehringer, U.; Lindner, B.; Seydel, U.; Rietschel, E. T.; Naoki, H.; Unger, F. M.; Imoto, M.; Kusumoto, S.; Shiba, T. Structure of de-O-acylated lipopolysaccharide from the Escherichia coli Re mutant strain F 515. *Tetrahedron Lett.* **1985**, *26*, 6321−6324.
(15) Helander, I. M.; Kilpelaeinen, I.; Vaara, M.; Moran, A. P.; Lindner, B.; Seydel, U. Chemical structure of the lipid A component of lipopolysaccharides of the genus Pectinatus. *Eur. J. Biochem.* **1994**, *224*, 63−70.
(16) Vinogradov, V.; Bock, K.; Holst, O.; Brade, H. The structure of the lipid A - core region of the lipopolysaccharide from Vibro cholerae O1 smooth strain 569B (Inaba) and rough mutant strain 95R (Ogawa). *Eur. J. Biochem.* **1995**, *233*, 152−158.
(17) Kastowsky, M.; Gutberlet, T.; Bradaczek, H. Molecular modelling of the three-dimensional structure and conformational flexibility of bacterial lipopolysaccharide. *J. Bacteriol.* **1992**, *174*, 4798−4806.

(18) Kastowsky, M.; Gutberlet, T.; Bradaczek, H. Comparison of X-ray powder-diffraction data of various bacterial lipopolysaccharide structures with theoretical model conformations. *Eur. J. Biochem.* **1993**, *217*, 771−779.
(19) Wistroem, C. A.; Jones, G. M.; Tobias, P. S.; Sklar, L. A. Fluorescence resonance energy transfer analysis of lipopolysaccharide in detergent micelles. *Biophys. J.* **1996**, *70*, 988−997.
(20) Labischinski, H.; Vorgel, E.; Uebach, W.; May, R. P.; Bradaczek, H. Architecture of bacterial lipid A in solution—a neutron small-angle scattering study. *Eur. J. Biochem.* **1990**, *190*, 359−363.
(21) Jung, S.; Min, D.; Hollingsworth, R. I. A Metropolis Monte carlo method for analysing the energetics and dynamics of lipopolysaccharide supramolecular structure and organization. *J. Comput. Chem.* **1996**, *17*, 238−249.
(22) Obst, S.; Kastowsky, M.; Bradaczek, H. Molecular dynamics simulations of six different fully hydrated monomeric conformers of Escherichia coli Re-lipopolysaccharide in the presence and absence of Ca^{2+}. *Biophys. J.* **1997**, *72*, 1031−1046.
(23) Hoess, A.; Watson, S.; Silber, G. R.; Liddington, R. Crystal structure of an endotoxin-neutralizing protein from the horseshoe crab, Limulus anti-LPS factor, at 1.5 A resolution. *EMBO J.* **1993**, *12*, 3351−3356.
(24) Morrison, D. C.; Jacobs, D. M. Binding of polymyxin b to the lipid A portion of bacterial lipopolysaccharide. *Immunochemistry* **1976**, *13*, 813−818.
(25) David, S. A.; Balasubramanian, K. A.; Mathan, V. I.; Balaram, P. Analysis of the binding of polymyxin B to endotoxic lipid A and core glycolipid using a fluorescent displacement probe. *Biochim. Biophys. Acta* **1992**, *1165*, 145−152.
(26) Cajal, Y.; Rogers, J.; Berg, O. G.; Jain, M. K. Intermembrane molecular contacts by polymyxin B mediate exchange of phospholipids. *Biochemistry* **1996**, *35*, 299−308.
(27) Amir, S.; Sasson, S.; Kaiser, N.; Meyerovitch, J.; Schechter, Y. Polymyxin B is an inhibitor of insulin-induced hypoglycemia in the whole animal model. Studies on the mode of inhibitory action. *J. Biol. Chem.* **1987**, *262*, 6663−6667.
(28) David, S. A.; Awasthi, S. K.; Wiese, A.; Ulmer, A. J.; Lindner, B.; Brandenburg, K.; Seydel, U.; Rietschel, E. T.; Sonneson, A.; Balaram, P. Characterisation of the interactions of a polycationic, amphiphilic, terminally branched oligopeptide with lipid A and lipopolysaccharide from the deep rough mutant of Salmonella minnesota. *J. Endotoxin Res.* **1996**, *3*, 369−379.
(29) Macura, S.; Kumar, N. K.; Brown, L. R. Combined use of COSY and double-quantum two-dimensional NMR spectroscopy for elucidation of spin systems in polymyxin B. *Biochem. Biophys. Res. Commun.* **1983**, *117*, 486−492.
(30) Liao, S. Y.; Ong, G. T.; Wang, K. T.; Wu, S. H. Conformation of polymyxin B analogs in DMSO from NMR spectra and molecular modelling. *Biochim. Biophys. Acta* **1995**, *1252*, 312−320.
(31) Bhattacharjya, S.; David, S. A.; Mathan, V. I.; Balaram, P. Polymyxin B nonapeptide: conformations in water and in the lipopolysaccharide-bound state determined by two-dimensional NMR and molecular dynamics. *Biopolymers* **1997**, *41*, 251−265.
(32) Srimal, S.; Surolia, N.; Balasubramanian, S.; Surolia, A. Titration calorimetric studies to elucidate the specificity of the interactions of polymyxin B with lipopolysaccharides and lipid A. *Biochem. J.* **1996**, *315*, 679−686.
(33) Dyson, H. J.; Wright, P. E. Defining solution conformations of small linear peptides. *Annu. Rev. Biophys. Biophys. Chem.* **1991**, *20*, 519−538.
(34) Wilmot, C. M.; Thornton, J. M. β-Turns and their distortions: a proposed new nomenclature. *Protein Eng.* **1990**, *3*, 479−493.
(35) Pristovšek, P.; Kidrič, J. NMR and molecular dynamics study of muroctasin—implications for the bioactive conformation. *Biopolymers* **1997**, *42*, 671.
(36) Nicklaus, M. C.; Wang, S.; Driscoll, J. S.; Milne, G. W. A. Conformational Changes of Small Molecules Binding to Proteins. *Bioorg. Med. Chem.* **1995**, *3*, 411−428.
(37) Clore, G. M.; Gronenborn, A. M. Theory and applications of the transferred nuclear Overhauser effect to the study of the conformations of small ligands bound to proteins. *J. Magn. Reson.* **1982**, *48*, 402−417.
(38) Gegner, J. A.; Ulevitch, R. J.; Tobias, P. S. Lipopolysaccharide (LPS) Signal Transduction and Clearance. *J. Biol. Chem.* **1995**, *270*, 5320−5325.
(39) Koch, P. J.; Frank, J.; Schuler, J.; Kahle, C.; Bradaczek, H. Thermodynamics and structural studies of the interaction of polymyxin B with deep rough mutant lipopolysaccharides. *J. Colloid Interface Sci.* **1999**, *213*, 557−564.
(40) Carpenter, C. L.; Cantley, L. C. A flattened face for membranes. *Nature Struct. Biol.* **1998**, *5*, 843−845.
(41) Schindler, M.; Osborn, M. J. Interaction of divalent cations and polymyxin B with lipopolysaccharide. *Biochemistry* **1979**, *18*, 4425−4430.
(42) Pleiss, J.; Fischer, M.; Schmid, R. D. Anatomy of lipase binding sites: the scissile fatty acid binding site. *Chem. Phys. Lipids* **1998**, *93*, 67−80.
(43) Lang, D. A.; Dijkstra, B. W. Structural investigationsof the regio- and enantioselectivity of lipases. *Chem. Phys. Lipids* **1998**, *67*, 115−122.
(44) Wang, Y.; Hollingsworth, R. I. An NMR Spectroscopy and Molecular Mechanics Study of the Molecular Basis for Supramolecular Structure of Lipopolysaccharides. *Biochemistry* **1996**, *35*, 5647−5654.
(45) Piantini, U.; Sorensen, O. W.; Ernst, R. R. Multiple quantum filters for elucidating NMR coupling networks. *J. Am. Chem. Soc.* **1982**, *104*, 6800−6801.
(46) Braunschweiler, L.; Ernst, R. R. Coherence transfer by isotropic mixing: application to proton correlation spectroscopy. *J. Magn. Reson.* **1983**, *53*, 521−528.
(47) Jeneer, J.; Meier, B. H.; Bachman, P.; Ernst, R. R. Investigations of exchange processes by two-dimensional NMR spectroscopy. *J. Chem. Phys.* **1979**, *71*, 4546−4553.
(48) Bothner-By, A. A.; Stephens, R. L.; Lee, J.; Warren, C. D.; Jeanloz, R. W. Structure determination of a tetrasaccharide: transient nuclear overhauser effects in the rotating frame. *J. Am. Chem. Soc.* **1984**, *106*, 811−813.
(49) Piotto, M.; Saudek, V.; Sklenar, V. Gradient-tailored excitation for single-quantum NMR spectroscopy of aqueous solutions. *J. Biomol. NMR* **1992**, *2*, 661−665.
(50) Gronenborn, A. M.; Clore, G. M. Conformation of NAD+ bound to yeast and horse liver alcohol dehydrogenase in solution. The use of the proton-proton transferred nuclear Overhauser enhancement. *J. Mol. Biol.* **1982**, *157*, 155−160.
(51) Dauber-Ogusthorpe, P.; Roberts, V. A.; Ogusthorpe, D. J.; Wolff, D. J.; Genest, M.; Hagler, A. T. Structure and energetics of ligand binding to proteins: Escherichia coli dihydrofolate reductase-trimethoprim, a drug-receptor system. *Proteins Struct. Funct. Genet.* **1988**, *4*, 31−47.

JM991031B